POAC'13
Espoo, Finland

Proceedings of the 22nd International Conference on
Port and Ocean Engineering under Arctic Conditions
June 9-13, 2013
Espoo, Finland

POAC13-166

ICE ISLAND DRIFT AND DETERIORATION FORECASTING IN EASTERN CANADA

G. Crocker [1], T. Carrieres[2], and H. Tran [2]

[1]Ballicater Consulting Ltd, Kingston, CANADA

[2] Canadian Ice Service, Ottawa, CANADA

ABSTRACT

In the past decade several ice islands have calved from the Petermann Glacier in north-west Greenland. Some of these have drifted as far south as the north-east coast of Newfoundland, and in 2012 a 950m long fragment was observed on the Grand Banks. Ice islands are several orders of magnitude larger than the icebergs that typically frequent these waters and may pose a threat to offshore activities in the region. Preliminary efforts at simulating ice island drift and deterioration have been conducted at the Canadian Ice Service. Theoretical analyses of deterioration mechanisms indicate that melting over the large upper and lowers surface areas can make significant contributions to overall deterioration. However, the 'thin plate' geometry of ice islands leads to the dominance of large scale fracture as a deterioration mechanism. The geometry and large size also result in changes in the relative importance of the various driving forces. The model physics suggest that wave radiation stress and pressure gradient forces are very important in controlling the drift of ice islands. The relative magnitudes of the component driving forces are presented here along with a discussion of why they differ from the key forces driving the drift of icebergs. Some preliminary results from the model hindcasts are also presented.

INTRODUCTION

Ice islands are massive pieces of glacial ice, usually protruding 5m or more above sea level, that have broken away from an Arctic ice shelf. They typically have thicknesses greater than 30m and areas of a few thousand square metres to 500 square kilometres or more (WMO 1970). The distinction between ice islands and icebergs is not absolutely clear, but in general they can be differentiated on the basis of origin, shape and size. Most importantly from a modelling and forecasting perspective ice islands have much larger lengths and widths than icebergs, but relatively small drafts.

In North America, ice islands are produced from ice shelves and large glaciers along the northern and western edge of the Arctic Archipelago (Koenig et al, 1952) and northern Greenland (Helk and Dunbar, 1953). During the past decade several calving events at the front of the Petermann Glacier (81°N, 62°W), in north-west Greenland, have introduced ice islands into Hall Basin (Peterson, 2011). Several of these features have been monitored as they drift southward, fracture, and melt, through a combination of satellite imagery and drift buoy deployments (Peterson et al, 2009).

A preliminary study of ice island drift and deterioration modelling has been conducted using a modified version of the North American Ice Service (NAIS) iceberg drift/deterioration model. The NAIS model was altered to account for ice island size and shape, and both theoretical predictions of the key drift forces and deterioration mechanisms are presented along with some comparisons of model results with the available observations.

OBSERVATIONS

Approximately 253km^2 of floating ice broke off the front of Petermann Glacier (81°N, 62°W) on 4 August 2010 (Falkner et al, 2011). A satellite tracking buoy was placed on the largest ice island fragment (PII-A) at about 78° 45' N by the Canadian Coast Guard on 18 September 2010 and transmitted position data for 253 days until it stopped operating on 26 May 2011. The drift track is shown on Figure 1. Three more buoys were deployed on PII-A by personnel from C-CORE and the University of Ottawa on 18 June 2011. The first 45 days of this transmission were available at the time the present analyses were conducted. This drift information is used here to assess the performance of the ice island drift model. In addition, time series of planar area of several of the fragments have been extracted for from satellite radar images (Desjardins, 2012, personal communication) and are used to assess deterioration rates.

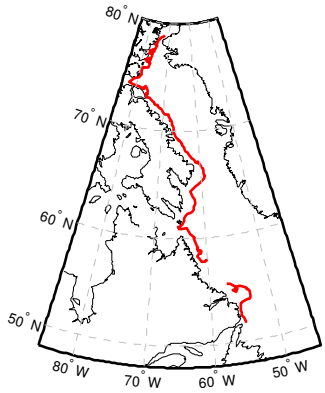

Figure 1. Map of PII-A drift track.

ICE ISLAND DRIFT MODEL

The original NAIS model for the drift/deterioration of *icebergs* has been we documented (Kubat et al, 2005; Kubat et al, 2007). The model is based on the conservation of momentum and conservation of mass,

$$m\frac{d\boldsymbol{u}}{dt} = \boldsymbol{F}_A + \boldsymbol{F}_W + \boldsymbol{F}_R + \boldsymbol{F}_C + \boldsymbol{F}_P + \boldsymbol{F}_{SI} \qquad (1)$$

where,

m = the iceberg mass including the added mass of water ($m = 1.5 \times m_{iceberg}$)
$\boldsymbol{u}$ = iceberg velocity (u and v components)
t = time
$\boldsymbol{F}_A$ = air drag force
$\boldsymbol{F}_W$ = water drag force
$\boldsymbol{F}_C$ = Coriolis force
$\boldsymbol{F}_R$ = wave radiation force
$\boldsymbol{F}_P$ = pressure gradient force
$\boldsymbol{F}_{SI}$ = sea ice force

For the *ice island model*, a number of changes were made to both the drift and deterioration components. These included some changes to model physics and some changes to the parameterizations used to approximate ice and environmental characteristics. The areas in which the ice island model differs from the iceberg model are described below.

Shape and Size

The primary distinguishing features of ice islands are their shape and size. Ice islands have relatively flat tops, nearly vertical sides and relatively flat bottoms (although this is less well documented). Their length-to-draft ratios are very large so they tend to retain this shape most of their life span. This makes modelling shape-related effects easier for ice islands than for icebergs. Observations by the authors indicate their planar shape can be reasonably represented as ellipses with a width (W) to length (L) ratio (k) of approximately 0.6. The projected sail area for form drag is a function of height above sea level (H) and length,

$$A_{sail} = H \cdot \sqrt{k \cdot L^2} \tag{2}$$

where the term under the square root is an average projected length for all orientations. On the east coast of Canada ice island height seems to fall into a fairly narrow range of between about 5m and 15m, so in the absence of observations a default value of H = 8m is used.

The keel area parameterization used in the iceberg model is based on iceberg underwater shapes and is not applicable to ice islands. Ice island draft is estimated empirically based on limited observations which suggest a typical draft to height ratio is 5.6:1 (Rudkin, Mueller, personal communications). Therefore the effective keel area is related to sail area by,

$$A_{keel} = 5.6 \cdot A_{sail} \tag{3}$$

Added Mass

Numerous authors (Shen and Ackley, 1991; Hopkins and Shen, 2001) note that bodies with large length/thickness ratios like sea ice floes have small added mass coefficients (C_m), but it becomes greater as the ratio decreases. The following parameterization was derived based on Rumer et al (1979), who performed model tests to determine the effect of ice floe aspect ratio (R_A = length/thickness ≈ L/D) on added mass.

$$C_m = 0.15 \qquad R_A \geq 15 \tag{4}$$

$$C_m = 0.73 \times R_A^{-1.64} + 0.15 \qquad 1.53 \leq R_A < 15 \tag{5}$$

$$C_m = 0.50 \qquad R_A < 1.53 \tag{6}$$

The shallow water on the Grand Banks may also have an effect on the added mass coefficient for ice islands (Croasdale and Marcellus, 1981; McTaggart, 1989) but the relationship appears to be complex and shape-dependent, so we have not included water depth effects at this stage.

Skin Friction

Since ice islands have very large, flat upper and lower surfaces, the drag forces due to skin friction may be significant. For small ice islands the skin friction forces are negligible. Since the draft of ice islands is assumed to be slowly varying and independent of length, the projected area for form drag increases linearly with length, but the upper and lower surface areas increase as the square of length. This causes a relatively rapid increase in surface area with length and correspondingly a rapid increase in the skin friction forces. The formulation used for air skin drag is,

$$F_{Askin} = \frac{1}{2} \cdot \rho_a \cdot C_{Askin} \cdot \frac{\pi}{4} (L \cdot W) \cdot \left| u_{a10} - U \right| \cdot (u_{a10} - U) \tag{7}$$

where ρ_a is the density of air, C_{Askin} is the skin drag coefficient, u_{a10} is the 10m wind velocity, U is the ice island velocity, and the term $(\pi/4)\cdot(L\cdot W)$ is the surface area assuming an elliptical shape. There is very little information on appropriate drag coefficients from undulating

surfaces typical of ice islands so as a first approximation we use a value of 0.0015 which is typical of sea ice. Skin friction on the bottom surface is,

$$F_{Wskin} = \frac{1}{2} \cdot \rho_w \cdot C_{Wskin} \cdot \frac{\pi}{4}(L \cdot W) \cdot \left| u_{wD} - U \right| \cdot (u_{wD} - U) \tag{8}$$

where ρ_w is the density of water, C_{Wskin} is the skin drag coefficient, and u_{wD} is the water velocity at depth D, the ice island draft. The skin drag coefficient was set to 0.004 based on Wadhams (2002).

Pressure Gradient Force

The pressure gradient (or sea surface slope) force is determined in the iceberg model as,

$$F_P = m \cdot \left(\frac{dV_w}{dt} + f \times V_w \right) \tag{9}$$

(Savage, 1999), where m is iceberg mass, V_w is the water velocity, and f is the Coriolis parameter,

$$f = 2 \cdot \Omega \cdot \sin \phi \tag{10}$$

and Ω is the earth's rate of rotation and ϕ is the latitude. Analyses of the forces generated in the ice island model revealed that this formulation produced very large and very irregular values of F_p, which should be a slowly varying parameter. Because the sea surface slope (α_s) was available as output from the ocean model it was decided to replace the existing equation with,

$$F_P = m \cdot g \cdot \sin \alpha_s \tag{11}$$

where g is acceleration due to gravity (Keghouche and others, 2009). This produced F_p values of similar magnitude and trend to the previous formulation but much more slowly varying.

ICE ISLAND DETERIORATION MODEL

The formulation for side wall deterioration follows very closely that of White et al. (1980) and Kubat et al. (2007). It has four components: buoyant vertical convection ($R_{bc(side)}$), forced convection ($R_{fc(side)}$), wave erosion ($R_{we(side)}$) and calving ($R_{calv(side)}$). The key difference is the adjustment of the formulae for the geometry of ice islands.

A parameterization for basal melting was required because of the relatively large area of the bottom surface. Assuming the bottom of the ice island is reasonably flat, its large lateral dimensions make it suitable for the application of heat transfer equations for turbulent flow over flat plates. The formulation is the same as that for forced convection melt of the sidewalls based on White et al. (1980) and yields the equation for the vertical (z) direction,

$$R_{fc(bot)} = 1.20 \cdot 10^{-5} \cdot (\Delta U_D + \bar{u}_D)^{0.8} \cdot \Delta T / (k \cdot L^2)^{0.1} \tag{12}$$

where ΔU_D is the ice/water differential velocity at the bottom of the ice island and the ice/water temperature differential (ΔT) is evaluated at depth D. The term $\bar{u}_D$ is the component of water velocity due to wave motion at depth D, and is a function of ocean wave frequency and length (see Ballicater, 2012 for details). Following Wadhams (1986) it is linearly added to the differential drift velocity.

A parameterization for melting at the upper surface was also added because of the relatively large surface area exposed to the atmosphere. Ignoring changes in heat storage in the ice, the energy available for melting at the upper surface of an ice island (Q) can be expressed as a

sum of the net radiative, sensible and latent heat fluxes. The melt rate ($R_{Q(top)}$) is the sum of component parts (Q) divided by $\rho_i \cdot \Gamma$, where ρ_i is the ice density and Γ is the latent heat of melting. This is applied vertically downward from the top surface and affects the thickness of the slab but has no effect on the lateral dimensions, except that draft and height are parameters in the side melt equations. A complete description of the radiative, sensible, and latent fluxes cannot be presented in the space available here, but they are based on established energy balance equations and documented in Ballicater (2012).

RESULTS

Drift Model

The predicted magnitudes of the different driving forces over a 3 day period in July 2011 are shown in Figure 2. Of particular note is the relative importance of the pressure gradient force and wave radiation stress, and the relatively small magnitudes of the form drag from air and water. This is a result of the size and shape. The pressure gradient force is large because of the large mass. The wave radiation force is large because the length of the ice island at the waterline (where the wave force is greatest) is very large in relation to its mass and other dimensions. The Coriolis force is at times large and fluctuates widely.

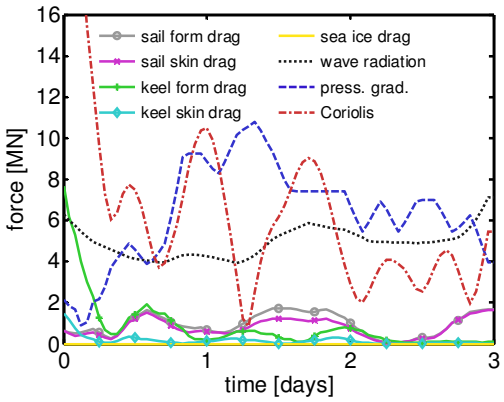

Figure 2. Driving force magnitudes, July 15 to 18, 2011 .

Figure 3 shows the observed drift of PII-A during a 24 day period in July 2011 (black dots) along with the 3-day hindcasts starting every 24 hours (red lines). The left side of the figure shows the complete drift track. This gives an overall impression that the hindcast drift is generally mimicking the observed drift. The right side of the figure shows the individual 3-day hindcasts. The scale is constant for all boxes. Here it is very evident that the drift speed, or equivalently the distance travelled over the 3-day period is grossly underestimated by the model. Also evident is that when the currents are strong, as in the early and later parts of the month, the hindcast drift direction is reasonable. However, the magnitude of the drift (the distance covered over the 72-hour period) is significantly under-predicted in most cases. When the currents are weak (the middle of the month) the hindcast directions and magnitudes are very poor.

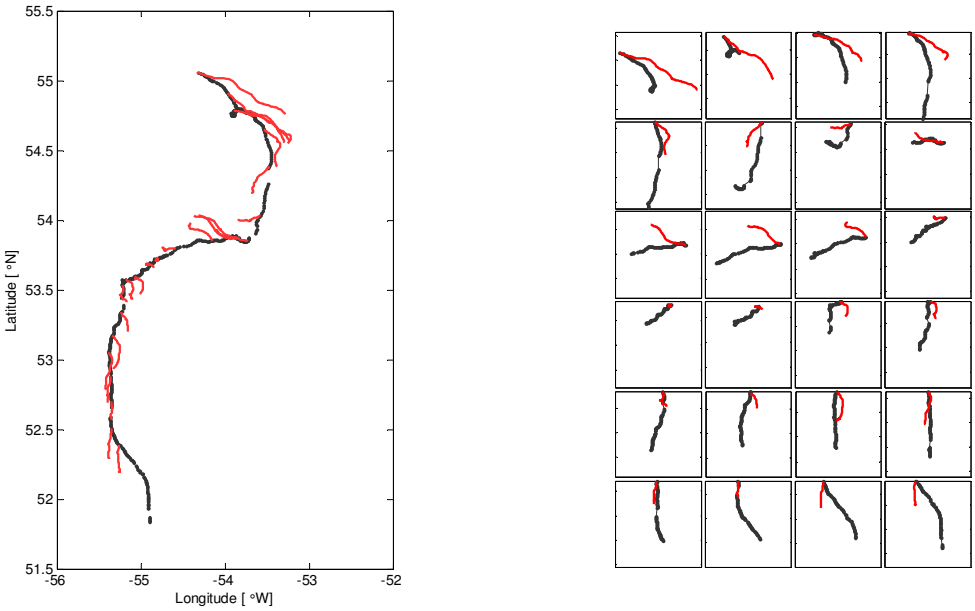

Figure 3. Observed (black) and hindcast (red) drift tracks for PII-A July 2011. The panels on the right show individual hindcasts with over the same 3-day hindcast periods.

Deterioration Model

To determine the relative importance of the various melting and calving processes to overall ice island deterioration a base case set of calculations were preformed. The values used are given in Table 1. They were chosen to represent a typical situation in the southern Labrador Sea or northern Grand Banks in spring time. The results are given in Table 2. Wave erosion of the keel and mass loss due to wave erosion and calving at the waterline combine to account for almost 80% of total deterioration. This is similar to the values reported by Savage (1999). In the base case, melting of the upper and lower surfaces is modest; accounting for a combined 13% of total deterioration, but will be shown below to become significant for larger ice islands.

Table 1. Base case values for deterioration analysis.

Ice Island		**Water**		**Atmosphere**	
L	= 1000 m	h	= 2.0 m	T_a	= 8.0 °C
W	= 600 m	τ	= 6.25 s	T_s	= 0.0 °C
H	= 8.0 m	ΔT	= 5.0 °C	ΔU	= 0.2 m/s
D	= 50.0 m	T_D	= 1.0 °C	u_{a10}	= 10.0 m/s

To investigate the effect of individual parameter values on the deterioration estimates, 3 sensitivity cases were run. The effects of length (L), wave height (h) and water temperature (ΔT) are show in Figure 4. In all cases the wave erosion accounts for a significant proportion of melt. The surface and basal melt can account for a large proportion of total melt for large ice islands, but the mass loss is spread over a very large surface area so the resulting change in thickness is still small. The relative importance of wave erosion at the waterline decreases with increasing wave height only because wave erosion over the entire sidewall increases much more quickly in high seas.

Table 2. Relative importance of deterioration processes.

Process	Variable Name	Volume [m^3/day]	Volume [% of total]	Linear Erosion [m/day]
Buoyant Convection	$R_{bc(side)}$	7,682	3.0	0.141
Wave Erosion	$R_{we(side)}$	148,832	58.6	2.72
Forced Convection (side)	$R_{fc(side)}$	11,783	4.6	0.217
Calving	$R_{calv(side)}$	52,548	20.7	0.962
Forced Convection (bottom)	$R_{fc(bot)}$	19,021	7.5	0.040
Surface Ablation	$R_{Q(top)}$	14,021	5.5	0.030

When the wave height is very small wave erosion over the entire sidewall is relatively small (this is the only case in which it is not the dominant deterioration mechanism). Waterline wave erosion on the other hand is still significant due to the large mass that can be removed by calving over a wave notch and the effectiveness of small waves, which are assumed to be of high frequency, in creating a notch. Water temperature effects are relatively small except near the freezing temperature. In very cold water the upper and lower surface melting are important, but waterline wave erosion quickly increases in relative importance as the water temperature increases.

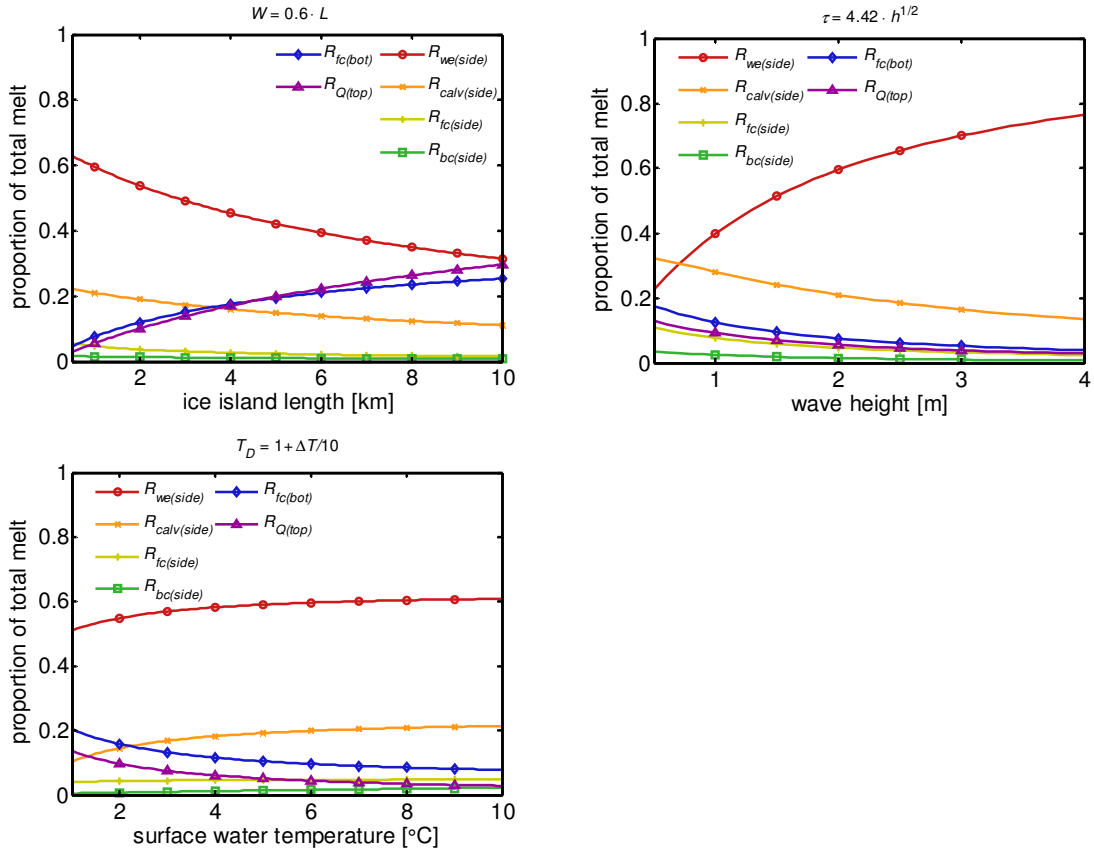

Figure 4. Effects of ice island length (upper left), wave height (upper right) and water temperature (lower left) on deterioration components.

A time series of ice island deterioration observations is available from Robe et al. (1977) who provided data on the surface plane area of an ice island that drifted onto the Grand Banks in 1976. The measurements were made from aerial photographs taken on May 12, 13, 31, and June 4 and 6. The water temperature was reported to be between 2 and 4°C, and El-Tahan et al. (1987) give average historical values for wave height, wave period and wind speed at this location and time of 1.5m, 7s, and 7.5m/s respectively. The freeboard of the ice island was reported as between 4 and 5m. The width to length ratio (k) was measured from the images as 0.43.

By scaling the reported surface areas from the Robe et al. (1977) photographs to obtain a linear scale, the length of the ice island on May 12 was estimated to be 751m and reduced to about 636m by June 6; a length change of 115m. Based on the elliptical model with the reported change in surface area and the observed value of k, the hindcast change in length was 143m. So in terms of length the model slightly over-predicted deterioration.

The time series of observed and modelled area are shown in Figure 5 (left side). In this case the model (solid line) produces reasonable correspondence with observations (dashed line with squares), but slightly under-predicts the change in area near the end of the observation period. This is a result of the progressive enlargement of small embayments due to the local concentration of wave energy (Robe et al., 1977), which reduced the surface area significantly without significantly affecting the length.

The modelled change in the thickness of the ice island over 25 days was 4.5m. There are no observations with which to compare with this number. It is important to note that there were no major splitting events during the observation period, but it appears on the last photograph in the series that a significant splitting event was about to take place. As described below, the effect of large scale fracture of ice islands on overall deterioration rates is significant.

Figure 5 also shows the time series of observed area of PII-A (dashed line with squares) during the month of July, 2011, along with that predicted by the model (blue line). The deterioration model significantly under-predicted the reduction in area. In this case the observed reduction in area was about 5 times that predicted by the model.

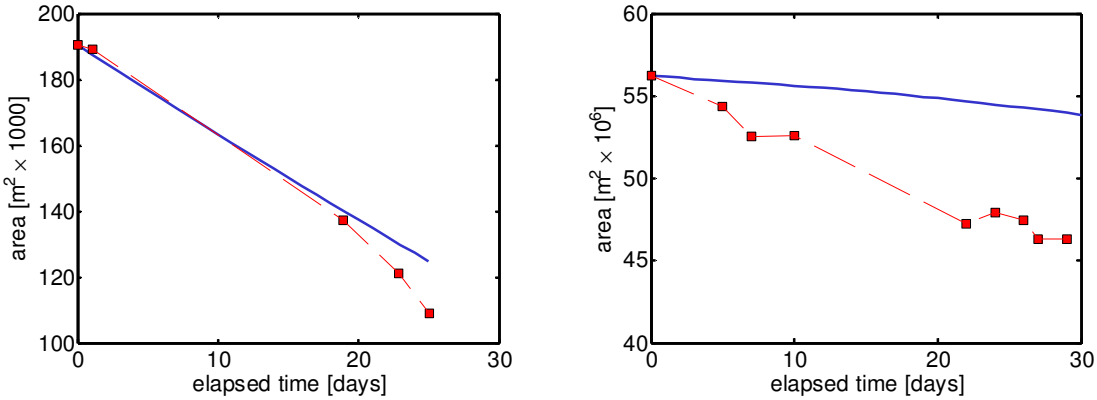

Figure 5. Observed and modelled deterioration of ice islands from Robe (1977) May 12 – June 6, 1976 (left) and PIIA, July 1 – 30, 2011 (right).

Figure 6 shows the planar area of ice islands PII-A, PII-B, and PII_B(a) extracted from RADARSAT imagery during the period September 2010 to August 2011 (Desjardins, personal communication, 2012). PIIA was deteriorating more quickly than the other two fragments during the summer period, but visual inspection of the satellite images revealed that all three were experiencing significant size reductions due to large scale fracture. These

fractures sometimes resulted in large sections of the 'plate' breaking off, and sometimes of the ice islands breaking into two large fragments. This mechanism of deterioration is not simulated in the deterioration model, but is at times the dominant deterioration mechanism.

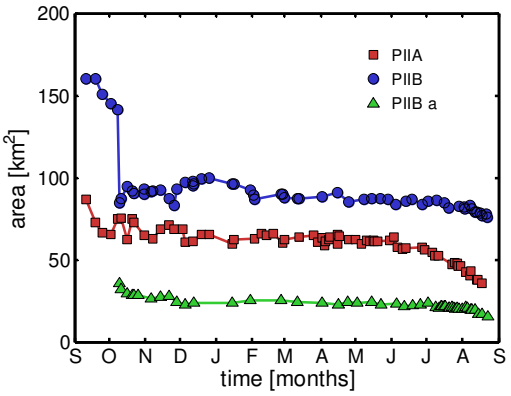

Figure 6. Time series of ice island planar area from satellite imagery.

CONCLUSIONS

Hindcasts of ice island drift have been performed with a version of the NAIS iceberg model with modified geometry and some small changes to model physics. Although the ice island model produced slightly better hindcasts than the unaltered iceberg model (not demonstrated here, see Ballicater, 2012 for details), the performance of the ice island drift model is still poor. Ocean currents are the key driving force and improved current forecasts are required if substantially better ice island drift forecasts are to be achieved. The hindcasts tended to under-predict the speed of drift. The observed ice island drift tracks show very little in the way of high frequency motions (the drift tracks are quite smooth). This suggests that a hybrid model that uses current information along with some sort of auto-correlation or damping function might lead to better results.

The ice island deterioration model described here incorporates melting on the upper and lower surfaces which can account for significant portions of overall mass loss due to melting. It has been shown to produce reasonable results for short term forecasts, over periods in which large scale fracture events do not occur. However, overall ice island deterioration is at times dominated by large scale fracture. Explicit prediction of this phenomenon is very difficult if not impossible on an operational basis. In future a semi-empirical approach, probably incorporating water temperature, may prove more effective.

ACKNOWLEDGEMENTS

Luc Desjardins provided valuable information on the drift and properties of the Petermann Ice Island fragments. Work-term students, Jennifer Ikert, and Lindsay Fleetwood performed all of the model hindcasts.

REFERENCES

Ballicater, 2012. Ice Island and Iceberg Studies 2012. Contract Report for Canadian Ice Service, Environment Canada, Ballicater Report 12-01.

Croasdale, K., and Marcellus, R. 1981. Ice Forces On Large Marine Structures, IAHR Symposium, Quebec City, pp. 755 – 770.

El-Tahan, M., Venkatesh, S., and El-Tahan, H. 1987. Validation and quantitative assessment of the deterioration mechanisms of Arctic icebergs, Journal of Offshore Mechanics and Arctic Engineering, 109:102-108.

Falkner, H. and 11 others. 2011. Context for the recent massive Petermann Glacier calving event, EOS, Transactions of the American Geophysical Union, 92(14):117-118, 5 April 2011.

Helk, J. and Dunbar, M., 1953. Ice Islands: evidence from north Greenland, Arctic, 6: 263-271.

Hopkins, M., and Shen, H. 2001. Simulation of Pancake-Ice Dynamics in a Wave Field. Annals of Glaciology, 33, 355-360.

Keghouche, I., Bertino, L., and Lisæter, K. 2009. Parameterization of an iceberg drift model in the Barents Sea, Journal of Atmospheric and Oceanic Technology, 26:2216-2227.

Koenig, L., Greenaway, K., Dunbar, M., and Hattersley-Smith, G., 1952. Arctic ice islands, Arctic, 5(2): 66-103.

Kubat, I, Sayed, M, Savage, SB, and Carrieres, T., 2005. An operational model of iceberg drift, International Journal of Offshore and Polar Engineering,15(2): pp 125-131.

Kubat, I., Sayed, M., Savage, S., Carrieres, T., and Crocker, G., 2007. An operational iceberg deterioration model, Proceedings of the 16th International Offshore and Polar Engineering Conference, Lisbon, Portugal, July 1-6, 2007.

McTaggart, K. 1989. Hydrodynamics and Risk Analysis of Iceberg Impacts with Offshore Structures, PhD thesis, University of British Columbia, 246 pp.

Peterson, I., Prinsenberg, S., Pittman, M., and Desjardins, L., 2009. The drift of an exceptionally-large ice island from the Petermann glacier in 2008, POAC'09, Luleå, Sweden, June 9-12, 2009, Paper 130.

Peterson, I. 2011. Ice island occurrence on the Canadian east coast, POAC'11, Proceedings of the 21st International Conference on Port and Ocean Engineering under Arctic Conditions, Montreal, Canada, July 10-14, 2011, Paper 44.

Robe, R., Maier, D., and R. Kollmeyer, 1977. Iceberg deterioration, Nature, 267:505-506.

Rumer, R., Crissman, R., and Wake, A. 1979. Ice Transport in Great Lakes. Contract Report Number 03-78-801-104, for Great Lakes Environmental Research Laboratory, National Oceanic and Atmospheric Administration, U. S. Department of Commerce.

Savage, S., 1999. Prediction of iceberg deterioration and drift – State of the art review. Contract Report for Canadian Ice Service, January 1999.

Shen, H., and Ackley, S., 1991. A one-dimensional model for wave-induced ice-floe collisions, Annals of Glaciology, 5, 87-95.

Wadhams, P., 2002. Ice in the Ocean. Gordon and Breach Scientific Publishers, London.
Wadhams, P., 1986. The seasonal ice zone. In: The Geophysics of Sea Ice, N. Untersteiner (ed.), NATO ASI Series B: Physics, Vol. 146, Plenum Press, New York.

White, F., Spaulding, M. and Gominho, L., 1980. Theoretical estimates of the various mechanisms involved in iceberg deterioration in the open ocean environment, Rep. CG-D-62-80, U.S. Coast Guard, Washington, D.C. 126 pp.

WMO, 1970. Sea-ice nomenclature. World Meteorological Organization, Geneva, Report 259.